Energy 102 (2016) 576–585

Contents lists available at ScienceDirect

Energy

journal homepage: www.elsevier.com/locate/energy

# Thermodynamic analysis and system design of a novel split cycle engine concept

Guangyu Dong*, Robert.E. Morgan, Morgan.R. Heikal

*School of Computing, Engineering and Mathematics, University of Brighton, BN2 4GJ, United Kingdom*

ARTICLE INFO

*Article history:*
Received 11 July 2015
Received in revised form
8 January 2016
Accepted 16 February 2016
Available online xxx

*Keywords:*
Split cycle engine
Isothermal compression
Waste heat recuperation
Isobaric combustion
System optimization

ABSTRACT

The split cycle engine is a new reciprocating internal combustion engine with a potential of a radical efficiency improvement. In this engine, the compression and combustion–expansion processes occur in different cylinders. In the compression cylinder, the charge air is compressed through a quasi-isothermal process by direct cooling of the air. The high pressure air is then heated in a recuperator using the waste heat of exhaust gas before induction to the combustion cylinder. The combustion process occurs during the expansion stroke, in a quasi-isobaric process. In this paper, a fundamental theoretical cycle analysis and one-dimensional engine simulation of the split cycle engine was undertaken. The results show that the thermal efficiency ($\eta$) is mainly decided by the CR (compression ratio) and ER (expansion ratio), the regeneration effectiveness ($\sigma$), and the temperature rising ratio (N). Based on the above analysis, a system optimization of the engine was conducted. The results showed that by increasing CR from 23 to 25, the combustion and recuperation processes could be improved. By increasing the expansion ratio to 26, the heat losses during the gas exchange stroke were further reduced. Furthermore, the coolant temperatures of the compression and expansion chambers can be controlled separately to reduce the wall heat transfer losses. Compared to a conventional engine, a 21% total efficiency improvement was achieved when the split cycle was applied. It was concluded that through the system optimization, a total thermal efficiency of 53% can be achieved on split cycle engine.



## 1. Introduction

The scientific and public awareness of environmental and energy issues from road transport has promoted research of advanced technologies particularly in highly efficient internal combustion engines [1–3]. Low carbon engine developments, often with waste heat recovery are important pathways to reducing overall societal CO2 emissions [1,4,5]. Inspection of the internal combustion engine heat balance indicates that the consumed fuel energy is distributed into roughly three equal portions; energy converted to useful work, energy transferred to coolant and energy lost through the exhaust gases [6–8]. Two complementary approaches can be taken to improve the overall efficiency of the engine; improvement of the fuel conversion efficiency and the recovery of waste thermal energy. Improvements to the base combustion system include VVA (variable valve actuation) and use of advanced fuel injection systems with intelligent control [9,10]. These approaches effectively increase the work recovery from the combustion products and reduce the exhaust temperature and associated losses. Losses to the environment through the engine coolant system can be reduced by adopting novel low temperature combustion strategies [11]. The second above mentioned approach uses an additional cycle to recover the thermal losses from the ICE (internal combustion engine) through (for example) a supplementary organic Rankine cycle to scavenge heat from the exhaust gases of the engine [12,13].

With all these improvements combined, the practical engine efficiency could approach the theoretical efficiency limit of the engine operating cycles. The thermodynamic cycle itself now becomes the bottleneck to further efficiency improvements. To achieve a step improvement in IC engine efficiency, a fundamental change to the thermodynamic cycle is required.

The concept of splitting the ICE cycle into separate cylinders is not new, and it was first described by Ricardo in 1908 [14] and developed further by Scudari leading to a laboratory demonstration engine running on gasoline [15]. An advanced cycle was proposed by Coney [16] for stationary applications that was predicted to achieve 60% break thermal efficiency. The proposed cycle utilised

* Corresponding author. Tel.: +44 7572370651.
*E-mail address:* g.dong@brighton.ac.uk (G. Dong).

http://dx.doi.org/10.1016/j.energy.2016.02.102
0360-5442/

**Nomenclature**

| | |
|---|---|
| $a$ | droplet surface area ($m^2$/kg) |
| atdc | after top dead centre |
| AFR | air fuel ratio |
| $C$ | isothermal index |
| CA | crank angle |
| $C_v$ | specific heat under constant volume |
| $C_p$ | specific heat under constant pressure |
| $CR$ | compression ratio |
| $ER$ | expansion ratio |
| EVC | exhaust valve close timing |
| EVO | exhaust valve open timing |
| $h$ | *enthalpy (kJ/kg))* |
| IVC | Intake valve close timing |
| IVO | Intake valve open timing |
| $k$ | isentropic exponent |
| $p$ | pressure |
| $Q_{LH}$ | Fuel heat release amount (kJ) |
| $Q_{RE}$ | recuperated heat (kJ) |
| $S$ | entropy |
| $T$ | temperature (K) |
| $T_{in}$ | Intake air temperature (K) |
| $T_{out}$ | Outlet air temperature (K) |
| $u$ | heat transfer coefficient |
| $V$ | volume |

*Greeks*

| | |
|---|---|
| $\gamma$ | specific heat ratio |
| $\sigma$ | regeneration effectiveness |
| $\eta$ | thermal efficiency |

*Subscripts*

| | |
|---|---|
| LH | fuel lower heating value |
| RE | heat recuperation |
| REJ | heat rejection |

isothermal compression through water spray cooling during the compression stroke and high pressure heat recovery through intra cylinder recuperation. Both concepts were taken to laboratory demonstration, but were not commercialised. In 2010, a new split cycle engine that uses liquid nitrogen to cool the compressor, exploiting both the latent and sensible heat of the cryogenic fluid was developed [17] which overcomes the difficulties of carrying a water handling system on a road vehicle.

Recently, a systematic analysis of split cycle engine is conducted by Dong et al. [18]. The results indicated that the efficiency improvement of a split cycle engine is attributed to a combination of isothermal compression and waste heat recuperation. Isothermal compression not only reduces the compression work, but also increases the temperature difference between the exhaust gas and compressed air. Then a significant percentage of the waste heat in the exhaust can be directly recuperated through the high pressure recuperation process and reutilised in the combustion cylinder. However, some key affecting mechanisms of the split engine thermal efficiency are not revealed yet. Consequently, the principles of split cycle engine system design and optimization is still need to be investigated. Concerning the structure of the split cycle engine, there are less design constraints on a split cycle engine compared to a conventional engine. On a conventional engine, the compression and expansion ratios are interlinked through the structure design of the engine. Also, the wall temperatures are almost the same in the compression and expansion strokes. These constraints can be eased on a split cycle engine. For example, a higher expansion ratio can be achieved on a split engine independent of the compression stroke increasing the potential expansion work through a Miller type cycle [19]. The decoupling of the compression and combustion stroke chamber temperatures means a hot combustion chamber, favourable for low heat loss, can be achieved without compromising the volumetric efficiency during the air induction.

In this paper, a thermodynamic analysis of the split cycle is conducted firstly to understand the potential of the cycle. Then the process of isothermal compression, isobaric combustion and heat recuperation processes are analysed to explore and optimise the split cycle engine system design. Based on the previous split cycle engine numerical and experimental data [16,20,21], an one dimensional engine model was constructed. And then the key operating parameters of the engine, including compression and expansion ratios and cooling temperature, are investigated. The paper concludes with a discussion on the potential of a split cycle engine for road transport and stationary applications.

## 2. Engine structure and operating mechanism

The schematic of the split cycle engine and the overall working process are shown in Fig. 1. The labels of each working stage and the symbols which representing the state of the working fluids are demonstrated as well. It can be seen that ambient air is pre-compressed in the turbocharger, and then transferred to the reciprocating isothermal compression cylinder. There are several solutions to achieve the quasi-isothermal compression on practical engines [22,23]. However, to avoid extra system complexity and redundant components, the air temperature is reduced using a water spray directly into the chamber in this research. By injecting a controllable quantity of water during the compression stroke, the air temperature is controlled resulting in a quasi-isothermal compression. At the end of the compression stage, the high-pressure two-phase water/air mixture is discharged to a phase separator and the water is removed from the charge and sent back to a water tank. The compressed air is then transferred to a

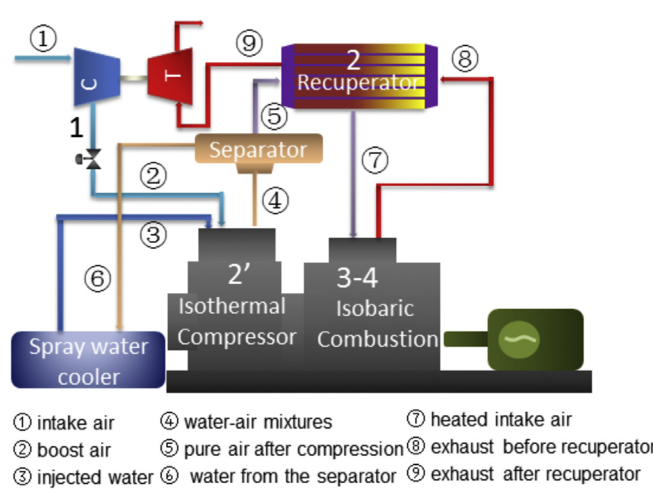


**Fig. 1.** Schematic of the 'isoengine' type Split cycle engine.

recuperator downstream of the separator. Within the recuperator, the high pressure air is heated by the exhaust gases, recovering thermal energy from the exhaust.

When the piston of the combustion cylinder reaches TDC (top dead centre), the intake valve of this cylinder opens for a very short time (typically less than 20° CA) and the preheated compressed air is fed to the combustion cylinder. As the fuel is injected after IVC (intake valve closing), combustion occurs during the expansion stroke of the cylinder. As a result, the combustion peak pressure is not increased significantly and a quasi-isobaric combustion process can be realised. At the end of the expansion stage, the cylinder pressure is very close to the pressure in the exhaust pipe, so the exhaust stroke can be assumed as nearly isobaric. Based on the above processes, a complete split cycle is achieved.

## 3. Thermodynamic cycle and parameter analysis

### 3.1. Thermodynamic cycle of the split cycle engine

The basic thermodynamic features of a split cycle engine are illustrated in the T–S diagram presented in Fig. 2. Referring to Section 2, both the combustion and exhaust strokes are assumed to be nearly isobaric, and the expansion stroke can be treated as nearly adiabatic [16]. However, the compressed air temperature in the real split cycle engine is reduced using a water spray directly into the chamber, and so the compression process can be considered as quasi-isothermal [20]. At the end of the compression process, the temperature of the compressed air $T_{2'}$ is strongly affected by the heat transfer process between the injected water and the intake air. To investigate the effect of heat transfer between air and water droplets on the $T_{2'}$, an equation derived from of the well-known relationship for an ideal gas undergoing isentropic compression or expansion is applied [24], expressed as:

$$\frac{T_{2'}}{T_1} = CR^{(K-1)\bullet\exp\left[-\frac{ua}{c_p}\left(1-\frac{T_w}{T_1}\right)\Delta t\right]} \tag{1}$$

Equation (1) describes the change of air temperature during a time interval $\Delta t$, with the exponential function representing the heat transfer to the water droplets. Within the exponential function, $T_w$ is the mean spray water temperature, $u$ is the heat transfer coefficient between the air and the water droplets and $a$ is the droplet surface area per unit mass of air. It should be noted this analysis only considers the absorption of sensible heat by the water droplets and the water is assumed to stay in the liquid stage. The validation of this equation can be seen in Ref. [16] and a detail modelling of the water–air heat transfer can be seen in Ref. [24]. If $ua\bullet\Delta t$ is near zero, there is almost no heat transfer between the water droplets and the air. So the air compression process can be treated as isentropic. Under such a condition the value of the exponential function tends to one and then Equation (1) is very close to the isentropic case. Conversely, if $ua\bullet\Delta t$ is large, then $T_{2'}$ rapidly converges to $T_w$ (normally $T_w$ is close to ambient temperature, $T_1$). In this case, the value of the exponential function tends to zero so $T_{2'}$ tends to $T_w$ and therefore approximately $T_1$. Since the exponential function is crucial in determining the temperature rise during the compression process, the parameter $C$ is defined as:

$$C = \exp\left[-\frac{ua}{c_p}\left(1-\frac{T_w}{T_1}\right)\Delta t\right] \tag{2}$$

In a real compression cylinder, the value of C is directly affected by the quantity and atomisation of the injected water. A higher water injection rate will lead to a lower C value, and then the compression process can be treated as nearly isothermal. The values of $T_{2'}$–$T_4$ can be expressed by the following equation:

$$\begin{aligned} T_{2'} &= T_1\cdot CR^{(K-1)\cdot C} \quad & T_3 &= T_2 + Q_{LH}/C_p \\ T_2 &= T_{2'} + Q_{RE}/C_p \quad & T_4 &= T_3/ER^{(K-1)} \end{aligned} \tag{3}$$

The recuperated heat $Q_{RE}$ is determined by both the exhaust temperature, which is influenced by the compression ratio CR and the fuel heat release $Q_{LH}$, and the performance of the recuperator. The recuperation effectiveness σ [25] can be defined as:

$$\sigma = \frac{H_2 - H_{2'}}{H_4 - H_{2'}} = \frac{T_2 - T_{2'}}{T_4 - T_{2'}} \tag{4}$$

It can be seen from Equation (3) that $T_{2'}$ trends towards $T_4$ with increasing recuperator effectiveness, σ. Then, the recuperated heat $Q_{RE}$ can be derived as:

$$Q_{RE} = \frac{Cp\cdot T_1\cdot\delta\cdot\left(1-ER^{(k-1)}\right)\cdot CR^{(k-1)\cdot C} + \delta\cdot Q_{LH}}{ER^{(k-1)} - \delta} \tag{5}$$

Thus, the net heat absorbed within the whole thermodynamic cycle is:

$$Q_{RE} + Q_{LH} = \frac{Cp\cdot T_1\cdot\delta\cdot\left(1-ER^{(k-1)}\right)\cdot CR^{(k-1)\cdot C} + ER^{(k-1)}\cdot Q_{LH}}{ER^{(k-1)} - \delta} \tag{6}$$

Heat is rejected in two strokes within the cycle; the exhaust stroke and the compression stroke. The exhaust stroke is assumed to be isobaric, so the heat rejection is $Q_{REJ} = C_p\bullet(T_4 - T_1)$. In the compression stroke, the intake air is compressed quasi-isothermally. As discussed earlier, this process can be treated as a polytrophic process with a polytrophic exponent C. So the rejected heat in this stroke is:

$$Q_{REJC} = \frac{Cv\cdot T_1\cdot(C-1)\cdot\left(CR^{(k-1)\cdot C}-1\right)}{C} \tag{7}$$

From Equations (4)–(6), the thermal efficiency of split cycle is given by:

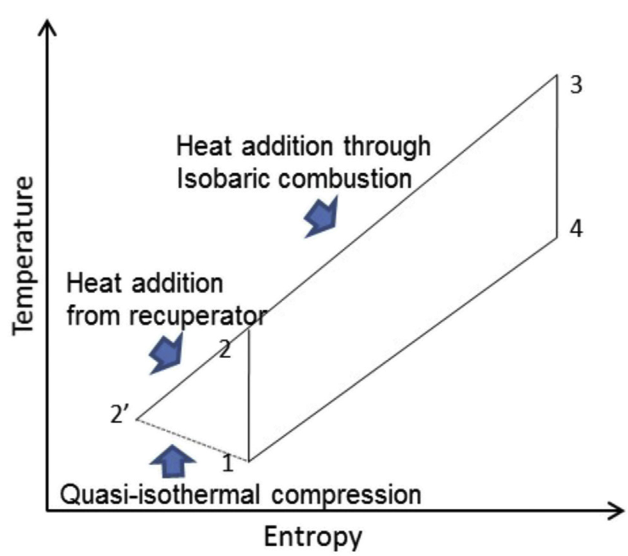


**Fig. 2.** T–S diagram of the split cycle.

$$\eta = \frac{(Q_{LH} + Q_{RE}) - (Q_{REJC} + Q_{REJE})}{Q_{LH}}$$
$$= \frac{ER^{(k-1)} - 1}{ER^{(k-1)} - \sigma} + \frac{Cp \cdot T_1}{Q_{LH} \cdot \left(ER^{(k-1)} - \sigma\right)} \cdot \begin{bmatrix} 2 \cdot \sigma \cdot CR^{(k-1)\cdot C} - \sigma \cdot ER^{(k-1)} \cdot CR^{(k-1)\cdot C} \\ -CR^{(k-1)\cdot C} + ER^{(k-1)} - \sigma \end{bmatrix} - \frac{Cv \cdot T_1 \cdot (C-1)}{C \cdot Q_{LH}} \left(CR^{(k-1)\cdot C} - 1\right) \tag{8}$$

An inspection of Equation (8) shows that the ideal thermal efficiency η is determined by 4 parameters: the CR/ER (compression/expansion ratio), isothermal index C, temperature rise ratio N (defined as $T_3/T_1$, representing the fuel release energy $Q_{LH}$) and recuperation effectiveness σ. This is different from the ideal thermal efficiency of conventional engines which is dominated by the compression ratio alone. In the following section, the influencing mechanism of these factors will be discussed. Based on the analysis result, the system design principles of split cycle engine will be studied.

### 3.2. Efficiency analysis of the split cycle engine

For conventional Otto cycle ICE, the ideal thermal efficiency is [26]:

$$\eta_{ideal} = 1 - \frac{1}{CR^{k-1}}$$

It can be seen that the compression ratio CR is the only design parameter which affects the efficiency, with higher values of CR resulting in higher efficiency. However, the efficiency of the split cycle engine is determined by the above mentioned 4 parameters. For comparing the conventional and split cycle engine efficiencies, a series of initial conditions were assumed based on a practical internal combustion engines, listed in Table 1 along with the other constant parameters applied for the split cycle analysis. In parallel, we assume the compression ratio CR is equal to the expansion ration ER for the split cycle in this section. Setting the recuperation effectiveness as 0.85 and a temperature rising ratio N to 6.5, the effect of CR value and isothermal index C on the cycle efficiency is shown in Fig. 3a.

The figure shows that the efficiency of the split cycle engine can reach 85% with an ideal isothermal compression process, which is much higher than that of an ideal ICE and in particular, achieves a higher efficiency at lower compression ratios. The efficiency is reduced for the quasi-isothermal compression case (C > 0) but is still higher than the Otto cycle case for low compression ratios. As mentioned in the previous section, a lower C value means the compression process is closer to isothermal. On a practical engine, the value of C can be reduced by increasing the amount of water injection during the compression process. For the C = 0.4 case, the efficiency of the split engine is higher than that of the conventional engine when the compression ratio CR is less than 16. However, there is no benefit for the split cycle engine when CR ≥ 16 as no heat can be recovered in the recuperation process. According to Equation (3), a higher compression ratio leads to a lower exhaust temperature (since CR = ER), and then the amount of recuperated heat decreases. As a result, the thermal efficiency of the split cycle engine will decrease when a higher compression ratio is applied. Under the condition of C = 0.2, the maximum efficiency is higher and the CR value below which heat recovery is possible is increased to 22. These concepts indicate that a larger recuperation range and a higher thermal efficiency can be achieved on the split cycle engine when the C value decreases and the compressor outlet temperature is close to $T_1$.

**Table 1**
Constants and initial conditions for the split cycle model.

| | | | |
|---|---|---|---|
| *General constants* | | | |
| k | $C_p$ kJ/(kg K) | $C_v$ kJ/(kg K) | |
| 1.38 | 1.001 | 0.721 | |
| $r_g$ kJ/(kg K) | $Q_L$ (J/g) | | |
| 0.28 | 44 000 | | |
| ***Initial conditions*** | | | |
| $T_1$ (K) | $P_1$ (bar) | | |
| 301 | 1.8 | | |
| ***Variables in the split cycle model*** | | | |
| CR | ER | C | δ |
| 0–30 | 0–30 | 0–1 | 0–1 |

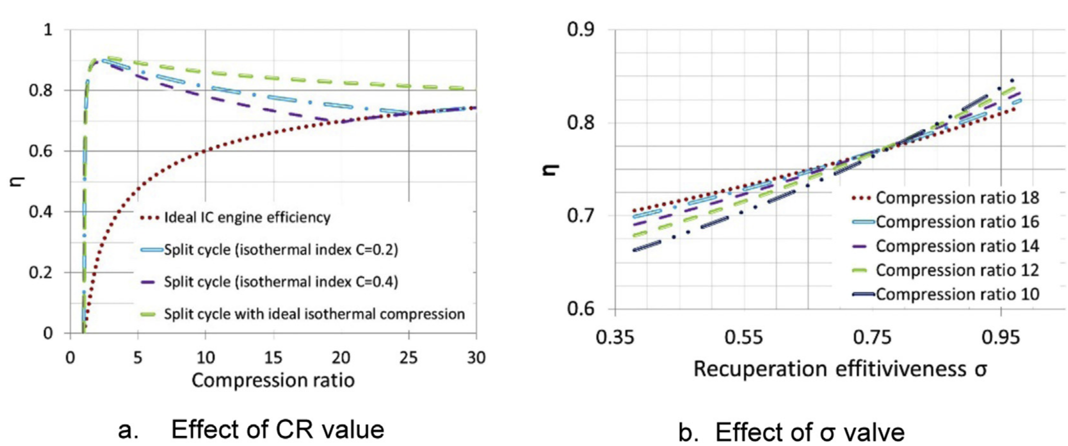


**Fig. 3.** Effect of (a) compression ratio and (b) recuperation effectiveness on thermal efficiency.

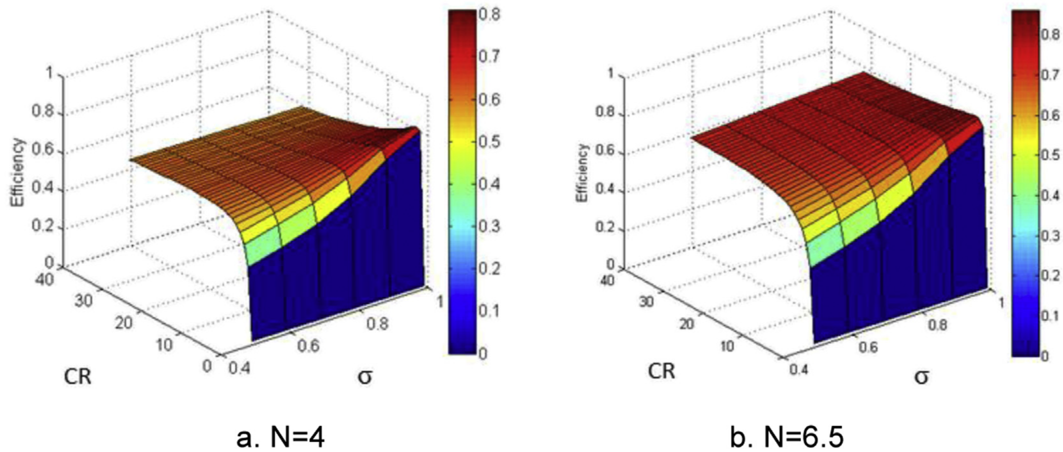


**Fig. 4.** Engine thermal efficiency MAPs under different temperature rising ratio conditions.

Fig. 3b demonstrates the effect of the recuperation effectiveness σ on the efficiency, η of the split cycle engine. It shows that η is higher when the σ increases under all compression conditions. When σ is less than 0.75, the compression ratio CR becomes the dominate factor on the thermal efficiency and the highest η is obtained when CR = 18. However, the effect of exhaust heat recuperation becomes dominate when σ ≥ 0.8. It can be seen that the highest η is achieved when CR = 10. This indicates that the heat recuperation process is crucial in delivering the high efficiency of the split cycle engine.

As well as the recuperation effectiveness, the fuel heat release $Q_{LH}$ also strongly affects the recuperation process and the engine efficiency. Given a fixed compression ratio, the temperature rise ratio N is determined by $Q_{LH}$. Fig. 4a and b shows performance maps under two temperature rise ratio conditions. The whole cycle efficiency is increased when N is raised from 4 to 6.5. This is mainly because a higher exhaust temperature enhances the exhaust heat recuperation process.

The above thermodynamic analysis indicates that a significant efficiency improvement can be achieved on a split cycle engine. Applying conventional engine dimensions and operation parameters (given CR = 17), the maximum η of an Otto and split cycle engines are 67% and 82% respectively.

The above analysis is based on conventional engine structure design. The constraints on conventional engines, such as bounded compression/expansion ratio and chamber wall temperature, do not exist on split cycle engines. By applying a higher compression ratio and keeping the expansion ratio ER constant, the peak combustion temperature $T_3$ can be increased. Meanwhile, the Temperature $T_4$ will not be decreased because of the unchanged ER value. To improve the cycle efficiency of a practical split cycle engine, a higher expansion ratio can also be applied to reduce the heat losses during the gas exchange stroke. The engine coolant temperature can also be controlled separately, giving the option to raise the combustion wall temperature and reducing heat losses during the expansion stroke. As the combustion event occurs during the expansion stroke, the peak combustion temperature is still lower comparing to conventional engines, but the mean temperature is higher. Also, the volumetric efficiency of the air intake will not be affected by the wall temperature. The coolant temperature of the expansion chamber can be increased to reduce the wall heat transfer losses. In the following section, the engine system design and optimisation will be discussed based on the results of a one dimensional engine model.

## 4. Engine system design and optimization

### *4.1. Engine modelling and experimental validation*

The theoretical analysis of the split thermodynamic cycle was discussed in the above section. However, the detail operating characteristics of a practical split cycle engine cannot be analysed

**Table 2**
Specifications and operating conditions of the modelled engines.

| | Conventional engine | Split cycle engine | |
|---|---|---|---|
| Stroke Type | 4 stroke | 2 stroke | ***Engine operating conditions:*** |
| Number of cylinders | 1 | 2 (1 combustor + 1 compressor) | Fuel type: Diesel |
| Compression ratio | 17 | 23 | Intake temperature: 25 °C |
| Bore [mm] | 128 | 128 | Intake pressure: 2.45 bar |
| Stroke [mm] | 148 | 148 | Coolant temperature: 80 °C |
| Intake valve opening (IVO) | 17° BTDC | 25° ATDC (compression chamber) 5° BTDC (expansion chamber) | Injected water temperature: 25 °C |
| Intake valve closing (IVC) | 174° BTDC | 174° BTDC (compression chamber) 10° ATDC (expansion chamber) | ***Working fluid:*** Air-fuel mixtures |
| Exhaust valve opening (EVO) | 172° ATDC | 5° BTDC (compression chamber) 172° ATDC (expansion chamber) | ***Recuperator specifications:*** Total length 600 mm |
| Exhaust valve closing (EVC) | 2° ATDC | 10° ATDC (compression chamber) 2° ATDC (expansion chamber) | Number of tubes: 35 |
| Engine speed [rpm] | 1500 | 1500 | Tube inner diameter: 4 mm |
| | | | Shell diameter: 35 mm |
| | | | Exhaust inlet location relative to intake: Opposite Side |

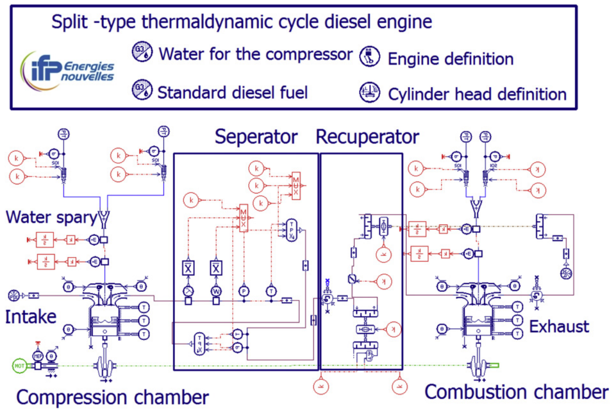


**Fig. 5.** Layout of the Split cycle engine model.

through the theoretical model. To optimise the engine structural/operating parameters, such as compression/expansion ratios and coolant temperatures, a one-dimensional engine model was developed and applied in this paper. The specifications and operating conditions of a conventional diesel engine and the engine applied split thermodynamic cycle are shown in Table 2. The key engine geometric characteristics are configured based on reference paper [18,20].

The LM Imagine.Lab AMESim [27] was used for the one-dimensional engine model development. Fig. 5 shows the layout of the proposed split cycle engine model. The cylinder in the left is the compression chamber. A spray heat transfer model in AMEsim 1-D engine package was integrated to simulate the effect of the water injection, and then validated by the experimental data from a prototype engine [21]. Then the quasi-isothermal compression of the intake air is well modelled.

Concerning the separator (as seen between the compression and the recuperator), there is no model template available in AMEsim environment. However, considering that the efficiency of commercial water separators is very close to 100%, we assumed that the water is completely removed from the air–water mixtures without changing the status of the flow transfer from the compression chamber to the recuperator. Thus, we assumed the composition of the gas flow to the recuperator is pure air, while the pressure and temperature of the recuperator inlet are exactly the same as the outlet air of the compression cylinder.

To predict the recuperation process, a recuperator component model was developed. The recuperator model was successfully in our previous work [17], and validated against established heat exchanger design software and theory [16]. Finally, the package IFP engine system is in particular devoted to the development of the diesel fuel combustion models [28]. Thus, the combustion process in the expansion chamber is achieved, and it was validated against experimental data collected on a conventional single cylinder diesel engine [18].

With a 1500 rpm engine speed and a fuel injection rate of 45 mg/cycle, a comparison between the Split cycle engine and the conventional diesel engine with the same structures is shown in Fig. 6a. For achieving the same level of combustion pressure, the compression ratio of the diesel engines and split cycle engine are set at 17 and 23 respectively. As shown in the figure, the pressure in the combustion chamber of the Split cycle engine increased dramatically when the intake valve opened, but the rate of pressure rise at the start of combustion was much lower compared to the conventional diesel engine, leading to a quasi-isobaric combustion process. The T–S diagrams of both engines can be seen in Fig. 6b. As a consequence of the quasi-isothermal compression and recuperation process, the area represents the available energy is much larger for the split cycle. The calculated efficiency of the conventional and split cycle engines were 39.7% and 48% respectively, which means that a 21% total efficiency improvement was achieved.

### 4.2. Effect of increased compression ratio

Unlike an Otto cycle engine, the thermodynamic analysis of the split cycle indicates that the engine thermal efficiency is not always increased when the compression ratio increases. On conventional engines, the compression is nearly adiabatic, and hence both temperature and pressure at TDC will be increased for a higher CR's. This can result in pre-ignition of fuel (for a spark ignited engine) and high firing pressures [29]. However, the compression process in split cycle engine can be considered as quasi-isothermal and a higher compression ratio will not lead to a higher temperature of the compressed air. So the compression ratio can be adjusted in a wider range to improve the thermal efficiency. Keeping the expansion ratio as 23 and the fuel injection rate as 45 mg/cycle, the effect of compression ratio on the cycle performance was analysed.

Fig. 7a shows the Log P–V diagrams of the engine under different CR conditions. It can be seen that the peak pressure in the expansion chamber increased when a higher CR was applied, so the output network increased. However, a higher CR value led to a higher exhaust temperature. Fig. 7b shows the temperature variation in the expansion chamber under these CR conditions. It can be seen that the expansion temperature $T_4$ in the chamber does decreased significantly when a higher CR value was applied.

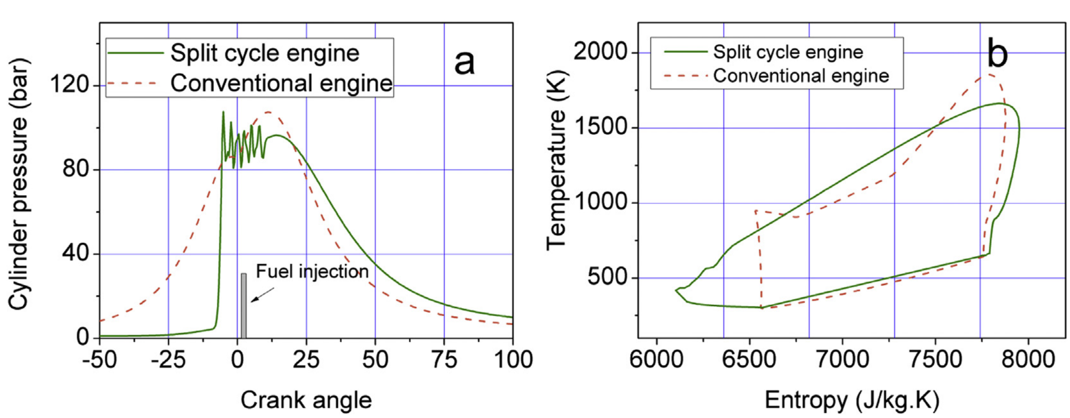


**Fig. 6.** Comparison of (a) cylinder pressure and (b) temperature-entropy variation between the Split cycle engine and diesel engine.

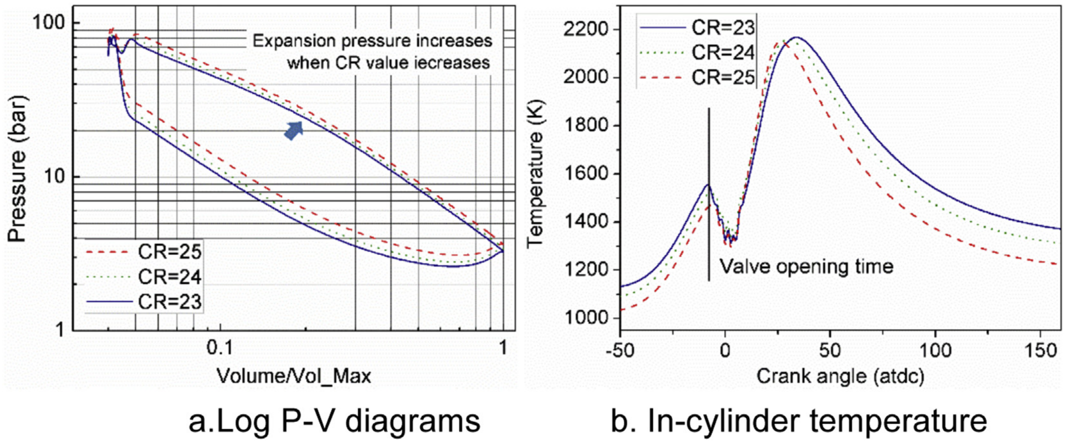


**Fig. 7.** Effect of compression ratio on (a) pressure-volume varying history and (b) in-cylinder temperature.

According to the equation: $Q_{REJE} = C_p \bullet (T_4 - T_1)$ in Section 3.1, this will lead to a higher heat losses during the gas exchange process. Consequently, the engine thermal efficiency will decrease through increasing the compression ratio.

Although the lower CR values led to higher thermal efficiency, the CR value must be sufficient to auto-ignite the fuel, in particularly under low load conditions where the intake air of the combustion chamber cannot be fully heated through the recuperation process. Hence, a VCR (variable compression ratio) system should be beneficial for improving the split cycle engine efficiency. The fuel formulation may also be a challenge for achieving the split cycle since the auto-ignition of the fuel may be difficult to achieve under lower CR conditions.

### 4.3. *Effect of increased expansion ratio*

The exhaust stroke is considered as isobaric in the ideal split cycle engine. In fact, limited by the stroke length, the exhaust pressure is higher than the ambient pressure on practical engines. This leads to energy losses in during the exhaust stroke. To resolve this problem, technologies such as VVA (variable valve actuation) is applied on conventional engines, and then a high expansion stroke can be achieved without affecting the compression ratio [30]. For the split cycle engine, the compression and expansion strokes are conducted in different chambers, and the ER and CR values can be adjusted independently. Thus, the effect of the expansion ratio on the efficiency is discussed in this section.

Keeping the CR value as 23, and increasing the fuel injection rate to 53 mg/cycle to demonstrate the variation of temperature $T_4$, the operating process in the expansion chamber under different ER conditions are illustrated using the T–S diagram in Fig. 8a. With increasing the expansion ratio, the exhaust stroke was closer to an isobaric process, which resulted in a reduction in the exhaust heat losses. In parallel, a higher ER value led to a lower exhaust temperature. Due to the recuperation process, both the peak temperature and the wall heat transfer in the expansion chamber were reduced as well.

Fig. 8b shows a comparison of the engine efficiencies under different ER conditions. When the ER value increased from 23 to 26, a 2.8% total efficiency improvement was achieved. Consequently, it can be deduced that a further efficiency improvement can be expected when a higher expansion ratio is applied to the split engine. However, the efficiency was reduced when the ER value increased to 27. Under such a condition, the pressure in the cylinder was much lower, which led to extra work losses.

### 4.4. *Separate cooling control system*

Heat transfer loss reduction is a key issue for improving the engine efficiency. By adjusting the coolant temperature, the cylinder wall and piston temperature can be raised resulting in a heat transfer loss reduction. However, the engine thermal load is also a concern at high coolant temperatures. In a conventional engine, the intake air is heated by the hot surface of the cylinder and the piston, and hence the air intake efficiency is reduced under high coolant temperature conditions. This issue does not affect the split cycle engine due to its separate chamber design. Thus, the wall

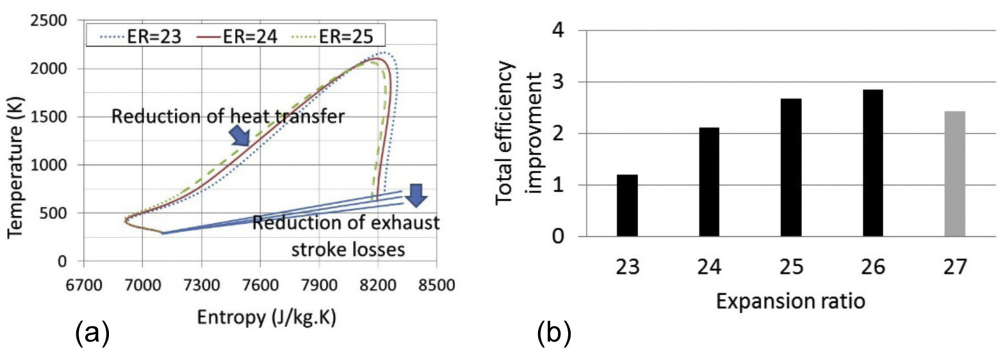


**Fig. 8.** Effect of expansion ratio on (a) temperature-entropy variations and (b) engine thermal efficiency.

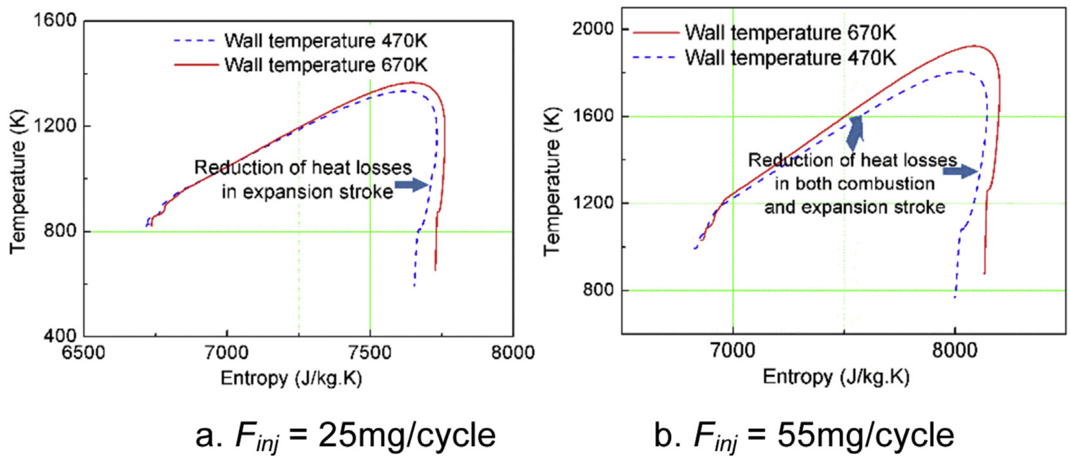


**Fig. 9.** Effect of coolant temperature on engine performance under condition of (a) $F_{inj}$ = 25 mg/cycle and (b) $F_{inj}$ = 55 mg/cycle.

**Table 3**
A steam-table of the flow properties in the optimized split cycle.

| Stream no. | ① | ② | ③ | ④ | ⑤ | ⑥ | ⑦ | ⑧ | ⑨ |
|---|---|---|---|---|---|---|---|---|---|
| Pressure (Mpa) | 0.098 | 0.18 | 45 | 8.89 | 8.54 | 8.62 | 8.67 | 0.35 | 0.098 |
| Temperature (K) | 301 | 383 | 301 | 351 | 342 | 351 | 638 | 762 | 301 |
| Mass flow (kg/h) | 16.65 | 16.65 | 41.2 | 57.85 | 16.48 | 41.2 | 16.48 | 17.32 | 17.32 |
| Volume flow ($m^3$/h) | 113.12 | 78.4 | 0.041 | 2.35 | 1.98 | 0.041 | 3.75 | 83.1 | 118.8 |
| Main Composition | (mole fraction) | | | | | | | | |
| $O_2$ | 0.21 | 0.21 | 0 | 0.046 | 0.21 | 0 | 0.21 | 0.045 | 0.045 |
| $N_2$ | 0.79 | 0.79 | 0 | 0.174 | 0.79 | 0 | 0.79 | 0.052 | 0.052 |
| Water ($H_2O$) | 0 | 0 | 1 | 0.78 | 0 | 1 | 0 | 0.046 | 0.046 |
| $CO_2$ (inc EGR) | 0 | 0 | 0 | 0 | 0 | 0 | 0 | 0.857 | 0.857 |

temperature of the expansion chamber can be adjusted by increasing the coolant temperature.

Maintaining the compression/expansion ratio at 23 and the fuel injection rate as 25 mg/cycle, the T–S diagram of the operating process in the expansion chamber is shown in Fig. 9a. A reduction of the heat transfer in the expansion stroke can be seen when the cylinder wall temperature increased. When the fuel injection rate was increased to 55 mg/cycle, the combustion temperature also increased. As seen in Fig. 9b, the heat loss from both the combustion and expansion strokes could be reduced by increasing the cylinder wall temperature from 470 K to 670 K. Such a result indicates that the engine efficiency can be improved through controlling the cooling system of compression chamber and expansion chamber separately. However, increases in combustion chamber temperature must not be at the cost of durability, particularly of the piston – liner lubrication system.

### 4.5. Systematic efficiency improvement of the split cycle engine

Based on the above modifications in Section 4.2–4.4, a significant efficiency improvement of the whole split cycle engine system can be achieved. A combined adjustment of the engine structural

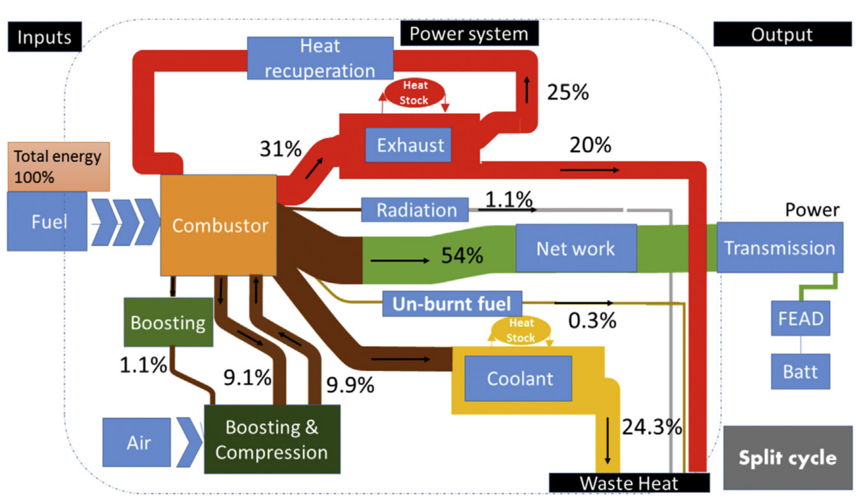


**Fig. 10.** The Sankey diagram of the split cycle engine energy flow.

parameters, including the compression/expansion ratio and the cylinder wall temperature, is conducted in this section. Setting the compression and expansion ratios to 24 and 26 individually, and increasing the wall temperature of the expansion chamber to 650 K, an improvement of the engine thermal efficiency is achieved. Referring to the location numbers in Fig. 1, the flowsheet which demonstrating the flow properties of the working fluids at each stages in the split cycle engine are shown in Table 3. Based on the table, an engine energy flow Sankey diagram can be worked out, as shown in Fig. 10. Through the diagram, the two key features of the split engine-the quasi-isothermal compression and the exhaust heat recuperation are clearly demonstrated. Also, the reason why the split cycle can be more efficient than the conventional Diesel cycle is illustrated. It can be seen that the amount of energy rejected to the environment is reduced, and the systematic engine thermal efficiency is improved. A comparison between the conventional diesel engine, the split cycle engine with conventional structure, and the optimized split cycle engine is shown in Fig. 11. Comparing to the split cycle engine with conventional structure, the percentage of regenerated energy was increased from 6% to 8%, and the heat transfer loss was reduced from 25% to 22% in the optimized split cycle engine. As a result, the engine efficiency was increased form 48% to 53% when the structure parameters were optimized. Compared with the baseline convention diesel engine at an efficiency of 39.7%, a total of 33% efficiency improvement can be expected on split cycle engines.

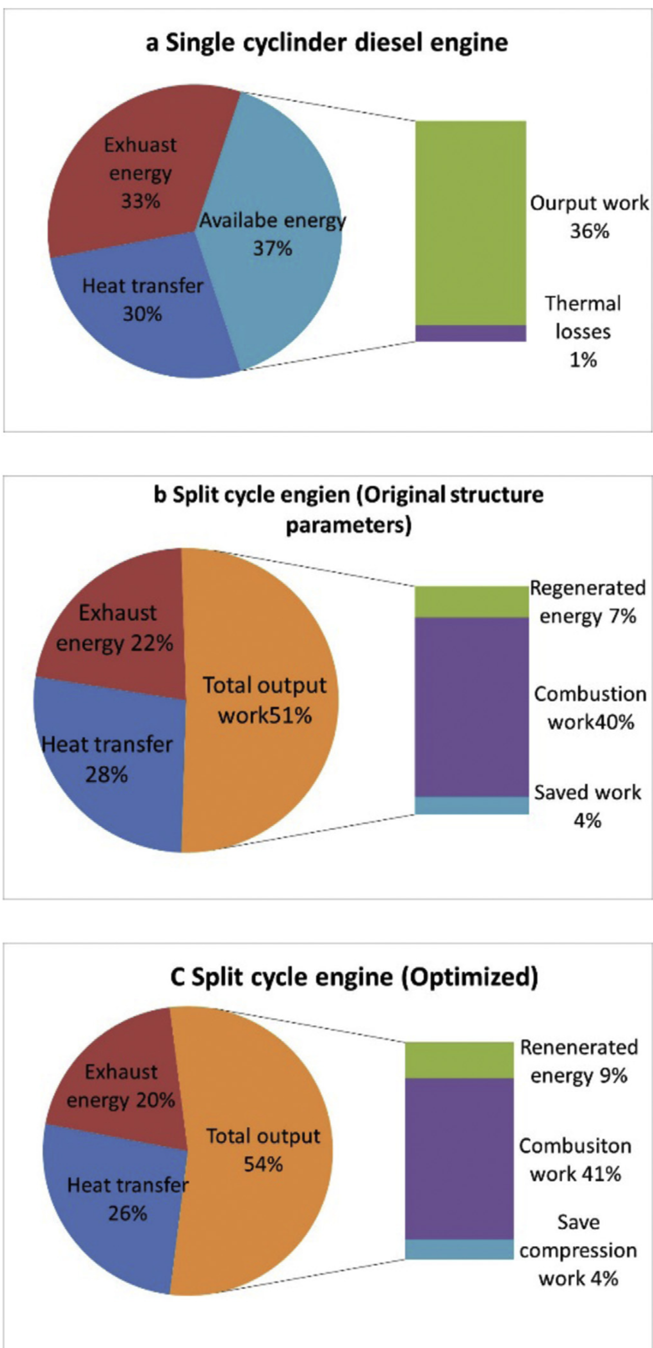


**Fig. 11.** Thermal efficiency improvement through the engine system optimization.

## 5. Conclusions

The fundamentals and performance of the split thermodynamic cycle are analysed in this paper. The initial study of engine system design and optimization is presented to explore the potential of the split cycle engine. The major findings of the study are as follows:

1) Unlike a conventional ICE, the efficiency of split cycle engine is determined by 4 key factors; the compression ratio, the expansion ratio, the recuperation effectiveness and the amount of heat release from the fuel.
2) Through the modelling analysis, the compression ratio of the split cycle engine is configure 24 to guarantee both the stable fuel auto-ignition and the higher thermodynamic efficiency. The expansion ratio is increased to 26 since a 2.8% total efficiency improvement still can achieved from over expansion.
3) Without affecting the volumetric efficiency of the compression cylinder, the wall temperature of the expansion cylinder can be raised to improve the engine efficiency. Especially, at higher load condition of fuel injection amount $F_{inj} = 55$ mg, the heat transfer losses in both combustion and expansion stroke are reduced if the wall temperature increases from 470 K to 670 K.
4) By applying a conventional engine structure, a 21% efficiency improvement can be achieved by the split cycle engine. Through the engine system optimization, the practical engine operation cycle can reach values close to the theoretical cycle, and a further 11% total efficiency improvement can be expected, raising the overall efficiency of the cycle to 53%.

## Acknowledgement

The research presented in this paper was funded by Innovate UK as part of the Crypower Project through the IDP8 technology program and EPSRC project 'Ultra Efficient Engines and Fuels' grant number EP/M009424. The authors would also like to thank LMS for providing an AMEsim licence under their academic support programme.

## References

[1] Saidura R, Rezaei M, Muzammil WK, Hassan MH, Paria S, Hasanuzzaman M. Technologies to recover exhaust heat from internal combustion engines. Renew Sustain Energy Rev 2012;16(8):5649–59.
[2] Saboori B, Sapri M, bin Baba M. Economic growth, energy consumption and $CO_2$ emissions in OECD (Organization for Economic Co-operation and Development)'s transport sector: a fully modified bi-directional relationship approach. Energy 2014;66:150–61.
[3] Noori M, Gardner S, Tatari O. Electric vehicle cost, emissions, and water footprint in the United States: development of a regional optimization model. Energy 2015;89:610–25.
[4] Lutsey N. Cost-effectiveness assessment of low-carbon vehicle and fuel technologies. Transp Res Rec 2010;2191:90–9.

[5] Hountalas DT, Mavropoulos GC, Binder KB. Effect of exhaust gas recirculation (EGR) temperature for various EGR rates on heavy duty DI diesel engine performance and emissions. Energy 2008;33(2):272–83.

[6] Mukai K, Miyazaki H, Yasuhara S. Measuring technique of the cooling loss and the influences of the operating variables on heat balance in a gasoline engine. 2003. p. 777–86. Vtms 6: vehicle Thermal Management Systems.

[7] Taymaz I. An experimental study of energy balance in low heat rejection diesel engine. Energy 2006;31(2–3):364–71.

[8] Lam N, Tuner M, Tunestal P, Andersson A. Double compression expansion engine concepts: a path to high efficiency. SAE Int J Engines 2015;8(4): 1562–78.

[9] Mamalis S, Babajimopoulos A, Guralp O, Najt PM, Assanis DN. The interaction between compression ratio, boosting and variable valve actuation for high load homogeneous charge compression ignition: a modeling study. Int J Engine Res 2014;15(4):460–70.

[10] Paden BA, Snyder S, Paden BE. Modeling and control of an electromagnetic variable valve actuation system. Ieee-Asme Trans Mechatronics 2015;20(6): 2654–65.

[11] Verschaerena R, Schaepdryvera W, Serruysa T, Bastiaenb M, Vervaekeb L, Verhelsta S. Experimental study of NOx reduction on a medium speed heavy duty diesel engine by the application of EGR (exhaust gas recirculation) and Miller timing. Energy 2014;76:614–21.

[12] Panesar AS, Morgan RE, Miché NDD, Heikal MR. Working fluid selection for a subcritical bottoming cycle applied to a high exhaust gas recirculation engine. Energy 2013;60:388–400.

[13] Dolz V, Novella R, García A, Sánchez J. HD Diesel engine equipped with a bottoming Rankine cycle as a waste heat recovery system. Part 1: study and analysis of the waste heat energy. Appl Therm Eng 2012;36:269–78.

[14] Arcoumanis C. Internal combustion engines. Combustion treatise, vol. x. London; San Diego: Academic Press; 1988. 397 pp.

[15] Sud K, Cetinkunt S, Fiveland SB. Modeling and validation of a split cycle clean combustion diesel engine concept. J Eng Gas Turbines And Power-Transactions Asme 2013;(8):135.

[16] Coney MW, Linnemann C, Abdallah HS. A thermodynamic analysis of a novel high efficiency reciprocating internal combustion engine – the isoengine. Energy 2004;29(12–15):2585–600.

[17] Jackson, N.S. and A.F. Atkins, Split cycle reciprocating piston engine. 2010, Google Patents, US8662030 B2.

[18] Dong GY, Morgan R, Heikal M. A novel split cycle internal combustion engine with integral waste heat recovery. Appl Energy 2015;157:744–53.

[19] Wu C, Puzinauskas PV, Tsai JS. Performance analysis and optimization of a supercharged Miller cycle Otto engine. Appl Therm Eng 2003;23(5):511–21.

[20] Coney MW, L.C., Greenwood AL, First test results of a novel large high-efficiency recip-rocating piston engine. Proceedings of the Fall Technical Conference of the ASME Internal Combustion Engine Division. ASME paper no. ICES2003-561(ICE-vol. 40): p. 409–418.

[21] Coney MW, L C, Morgan RE, Bancroft TG, Sammut RM. A novel internal combustion engine with simultaneous injection of fuel and pre-compressed pre-heated air. In: Proceedings of the fall technical conference of the ASME internal combustion engine division; 2002. p. 67–77. ASME paper no. ICEF2002-485(ICE-vol. 39).

[22] Iglesias A, Favrat D. Innovative isothermal oil-free co-rotating scroll compressor-expander for energy storage with first expander tests. Energy Convers And Manag 2014;85:565–72.

[23] Qin C, Loth E. Liquid piston compression efficiency with droplet heat transfer. Appl Energy 2014;114:539–50.

[24] Incropera FP, Incropera FP. Fundamentals of heat and mass transfer. 6th ed., vol. xxv. Hoboken, NJ: John Wiley; 2007. 997 pp.

[25] Ibrahim OM. Design considerations for ammonia-water Rankine cycle. Energy 1996;21(10):835–41.

[26] Heywood JB. Internal combustion engine fundamentals. McGraw-Hill series in mechanical engineering, vol. xxix. , New York: McGraw-Hill; 1988. 930 pp., 2 pp. of plates.

[27] Chen D, Sun R, Wu Y, Wang B. A Research on compressed natural gas engine fuel supply system for rapid prototyping based on AMEsim. Appl Energy Technol 2013;724–725:1317–23. Pts 1 and 2.

[28] Gu N, Ni JM. Simulation of engine cooling system based on AMESim. In: Icic 2009: second international conference on information and computing science, vol 4; 2009. p. 117–20. Proceedings.

[29] Ratnaweera A, Watson HC, Halgamuge SK. Optimisation of valve timing events of internal combustion engines with particle swarm optimisation. In: Cec: 2003 Congress on evolutionary computation, vols. 1–4; 2003. p. 2411–8. Proceedings.

[30] Bassett MD, Blakey SC, Foss PW. A simple two-state late intake valve closing mechanism. Proc Institution Mech Eng Part D-Journal Automob Eng 1997;211(3):237–41.